

Key words: articulated vehicles, crash modelling

WITOLD GRZEGOŹEK^{*)}, PIOTR ŚWIDER^{**)}, ANDRZEJ POLAŃSKI^{***)}

A NEW APPROACH TO CRASH MODELLING OF ARTICULATED LORRIES

The paper presents a plane model of articulated vehicles worked out for the analysis of their dynamics. The d'Alembert principle was used for derivation of motion equations for this system. The forces and moments acting on wheels were formulated on the basis of the Dugoff-Uffelman tyre model. The system consists of any number of vehicles connected by kinematic pair of the 5th class (non friction joint of pivot-bush type) and the fifth wheel (with dry friction). Since crash calculations usually take into account the impulse of crash force only, and since it is not appropriate for articulated vehicles, a new approach to crash calculation is presented in this paper. The authors propose to calculate the force in crash point both as a function of the relative velocity of vehicles and the stiffness of their bodies. Simulation results of articulated lorry crashes and the attempt to verify the performed simulation are presented in the article.

1. Physical model of a vehicle

In this paper the following ideas of creating physical model of articulated vehicle were proposed [1], [3], [5]:

- the considered system may consist of any number of vehicles joined by the 5th class kinematic pair (non friction joint of pivot-bush type) and the fifth wheel (with dry friction [4]),
- the model of each vehicle consists of the car body and any number of vehicle wheels [2].

^{*)} Cracow University of Technology, Institute of Automobiles and Internal Combustion Engines, Al. Jana Pawła II 37, 31-864 Kraków, Poland; E-mail: witek@mech.pk.edu.pl

^{**)} Cracow University of Technology, Institute of Automobiles and Internal Combustion Engines, Al. Jana Pawła II 37, 31-864 Kraków, Poland; E-mail: swider@mech.pk.edu.pl

^{***)} University of Bielsko-Biała, Department of Mechanics and Computer Engineering Methods, ul. Willowa 2, 43-309 Bielsko-Biała, Poland; E-mail: apolanski@ath.bielsko.pl

The motion of each vehicle in Oxy plane with right-handed coordinate system is described by three generalized coordinates that means $x^{(i)}$, $y^{(i)}$ of their centers of gravity $C^{(i)}$ and the $\psi^{(i)}$ angles of their rotation. Oxy plane can be arbitrarily sloped in relation to a horizontal plane. Movable coordinate systems $C^{(i)} x_C^{(i)} y_C^{(i)} z_C^{(i)}$ are fixed to the centres of gravity of each vehicle.

In Figure 1 the components of the tangent forces $F_{k_x}^{(i)}$, $F_{k_y}^{(i)}$ and the aligning moments $M_{S_k}^{(i)}$ were marked. The turn angles of the wheel in relation to the axis passing through geometrical centres $O_k^{(i)}$ and parallel to axis $C^{(i)} z_C^{(i)}$ are designated as $\delta_k^{(i)}$. A wheel of each vehicle may be loaded by driving torque $M_k^{(i)}$ or braking torque $M_{H_k}^{(i)}$. The interaction between “ i ” and “ $i + 1$ ” vehicles creates the forces R_{i_x} , R_{i_y} in a joint pair.

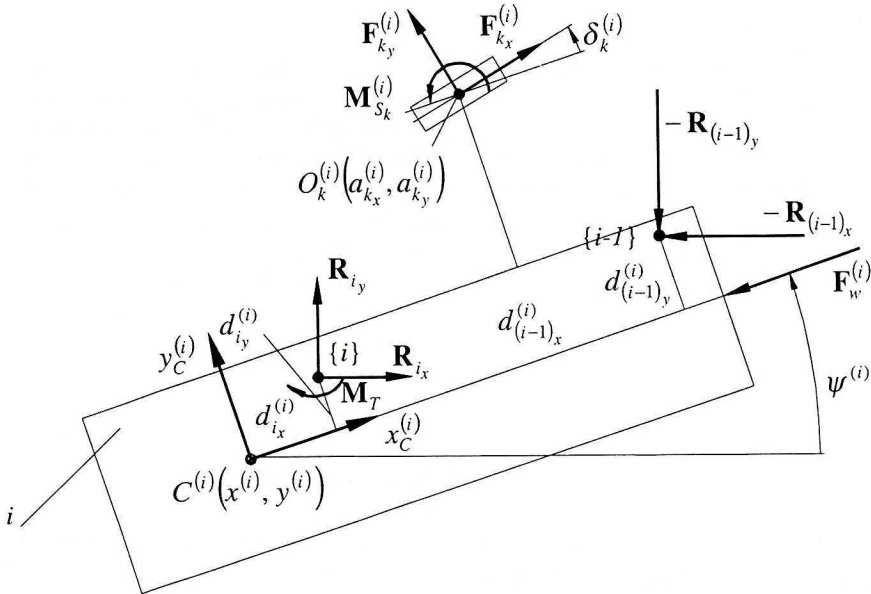


Fig. 1. Vehicle physical model with the 5th class kinematic pair, friction torque in fifth wheel and wind force taken into account

2. Mathematical model of a system

A physical model of an articulated vehicle system presented in this paper may be constructed of elements that make it possible to create any of its geometrical configuration. Individual elements of the physical model introduce unknown variables to the mathematical model. The elements of the model are subjected to the input variables in the following forms:

- vehicle gravity force,
- the force of aerodynamic drag,
- braking and driving torques acting on the wheels.

The elements of the model that constitute the considered vehicle unit are as follows:

- a vehicle with designated mass and mass moment of inertia to axis perpendicular to the motion plane,
- a rotary kinematic ideal pair joining two vehicles,
- wheel transfer forces and moments appearing in tire-road contact point,
- the fifth wheel this element transfers the loading force between the vehicles. Any spring elements located around the axis of rotation pair constitute this element. The loading forces generate the dry friction forces that act in the plane of the fifth wheel (Figure 2).

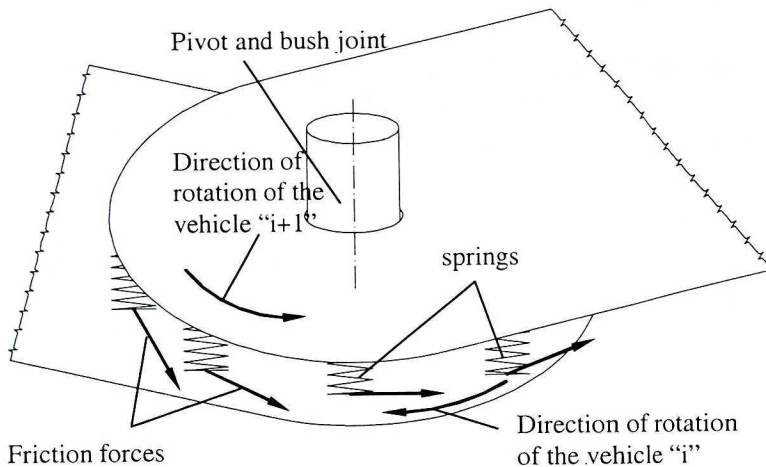


Fig. 2. The fifth wheel – the joint of a “i” vehicle and “i + 1” vehicle

In the model that is considered, friction can take two forms: kinetic and static that may cause the appearance of alternate phases- “stick together” and relative motion of the joined vehicle.

The forces occurring in joint pairs are calculated in each step of integration not only during the drive but also during the crashes. The step of integration during the crashes is significantly diminish.

3. Model verification

In order to verify the correctness of simplifications assumed in the model, two kinds of verification were carried out. The calculation results were

compared first with the experimental results and then with the numerical results obtained from a more sophisticated model worked out by S. Wojciech, I. Adamiec and W. Grzegożek [9].

Because there is a lack of experimental norms for articulated vehicles, the methodology used for personal cars was applied. The tested vehicle was the tractor Mercedes Actros 1840 LS Megaspaces with the semitrailer Kogel SN 24 P 100/1.060. The velocity of the vehicle was 60 km/h, and it was assumed that the turn angles of wheels were the same. The course of turn angle of the tractor front wheels measured during the test is presented in Figure 3. First, the results of simulation were compared with the experimental results. Afterwards, the simulation results were compared with the simulation results of a more complex model.

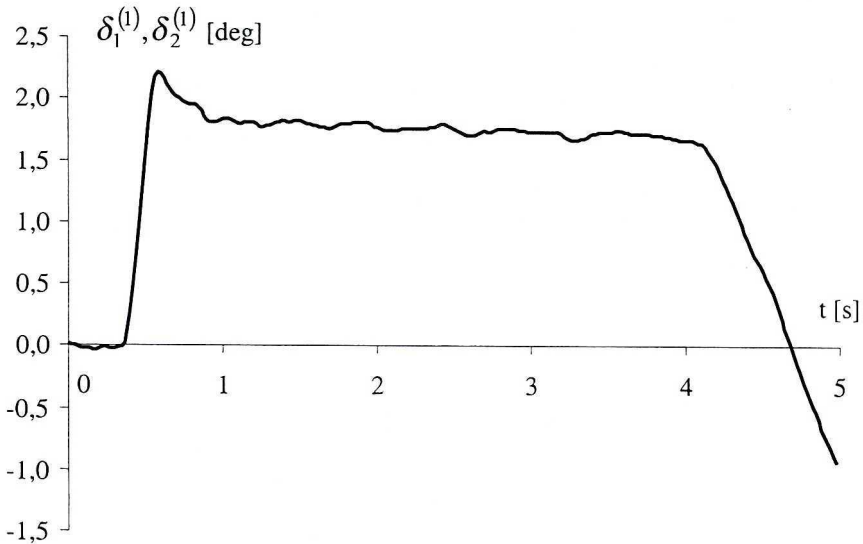


Fig. 3. The course of a tractor front wheels turn angle

Courses of yaw velocities for the tractor and the semitrailer are shown in Figures 4 and 5.

In Figures 4 and 5, thin lines represent results of road measurements, grey lines – calculation results of complex model [9], and thick lines denote calculation results of the model presented here.

The courses of yaw velocities for the tractor and the semitrailer measured and calculated by both methods differ only slightly. They have similar speed of increase and small difference in the steady state which is due to the difficulties in keeping constant speed of the vehicle during measurements.

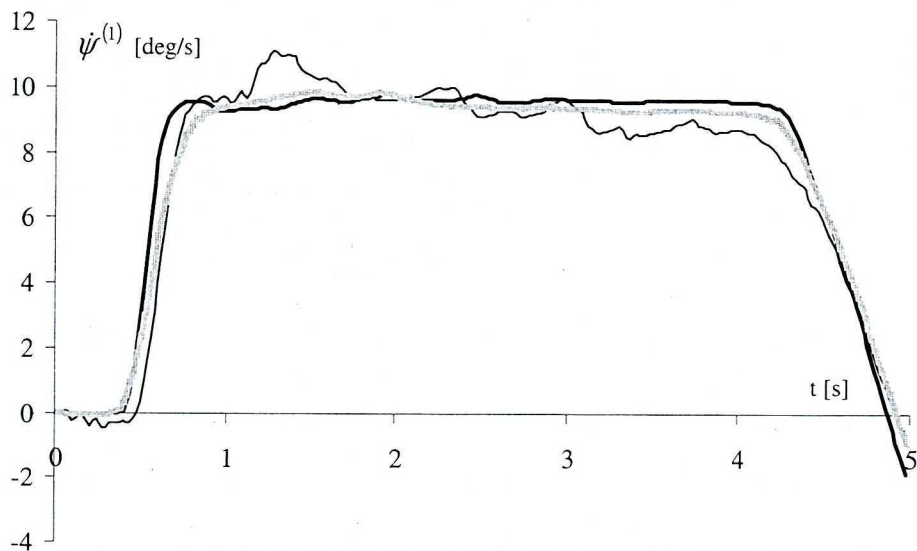


Fig. 4. Yaw velocity of a tractor

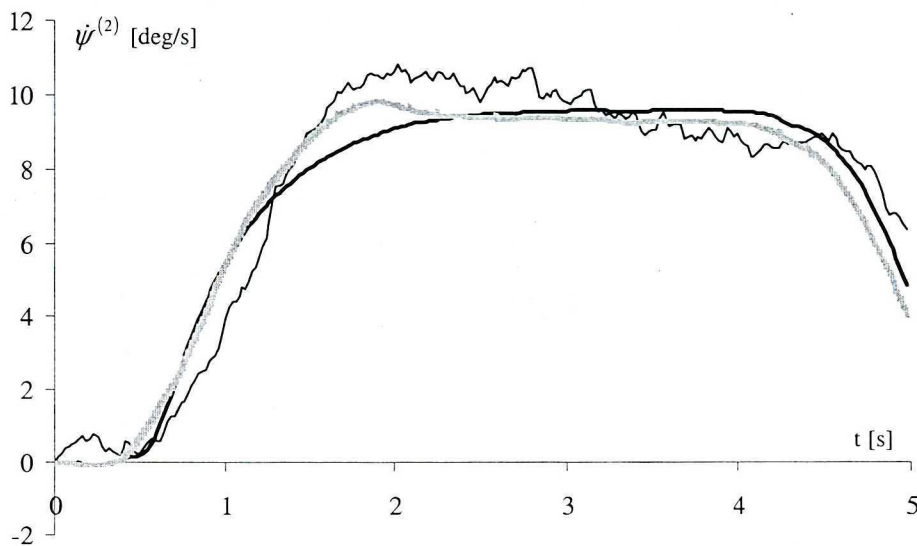


Fig. 5. Yaw velocity of a semitrailer

Second verification refers to articulated vehicle made of a truck joined with a trailer. Road measurements were carried out for the truck STAR 944 with the trailer Sanok D-50. The velocity of the truck

Table 1.

Percentage differences between the measurement results, calculation results, and the results obtained by calculation based on a model [9]

	Measurement results – calculation results		Measurement results – calculation results based on a model [9]		calculation results – calculation results based on a model [9]	
	For a tractor	For a trailer	For a tractor	For a trailer	For a tractor	For a trailer
The maximum difference with reference to the maximum value, in the steady state	16%	16%	13%	13%	4%	7%
The average difference with reference to the average value, referring to the complete run	9%	11%	7%	10%	4%	5%
The average difference with reference to the average value, in the steady state	6%	7%	5%	6%	2%	2%

was 40 km/h, and it was assumed that the turn angles of wheels were the same. The course of turn angles of the front wheels of the tractors measured during the test is presented in Figure 6.

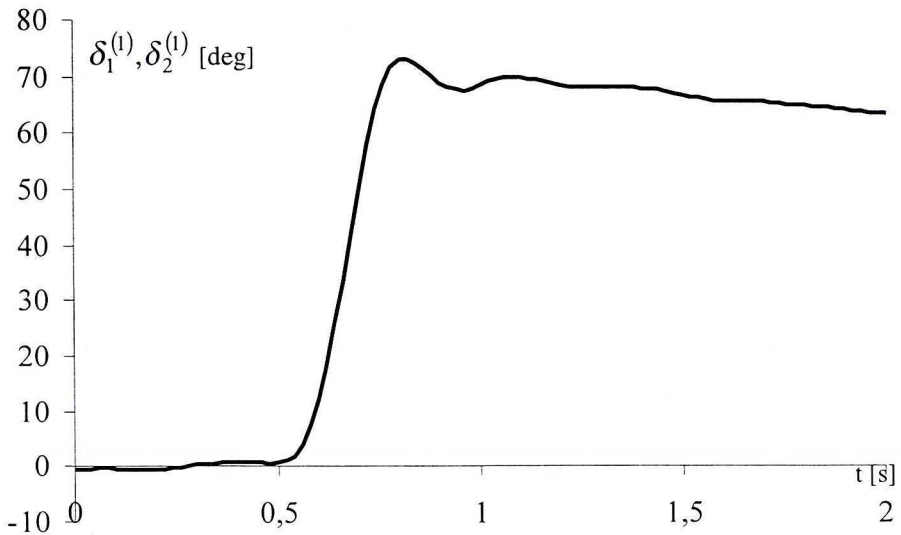


Fig. 6. The course of lorry front wheels turn angle

Results given as angular velocities of truck and trailer are presented in Figures 7 and 8.

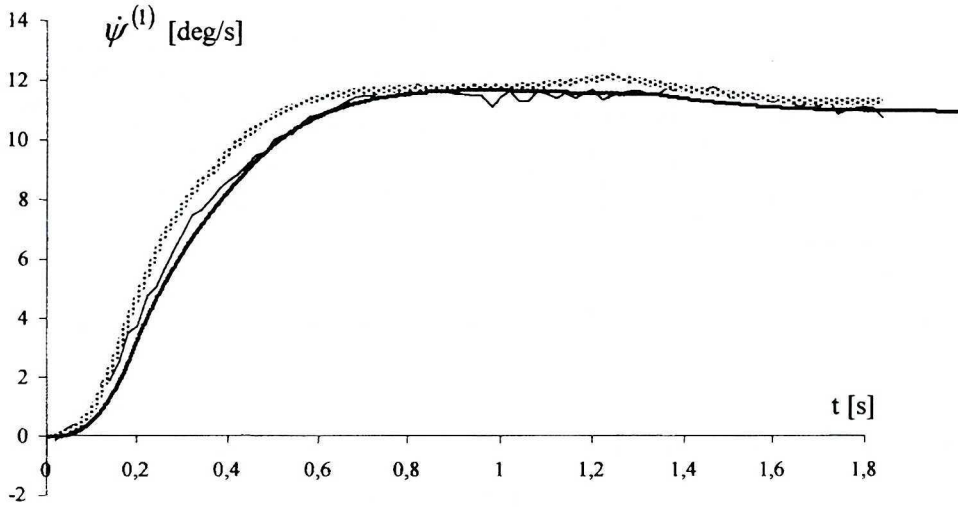


Fig. 7. Yaw velocity of a lorry

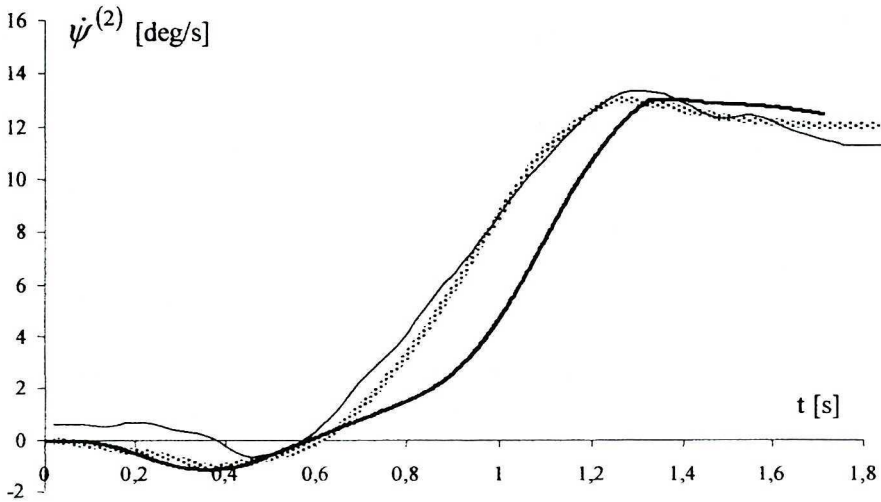


Fig. 8. Yaw velocity of a trailer

In Figures 7 and 8, thin lines represent the results of road measurements, grey lines calculation results of complex model [9], and thick lines are calculation results of the model presented here.

Table 2.

Percentage differences between the measurement results, calculation results, and the results obtained by calculation based on a model [9]

	Measurement results – calculation results		Measurement results – calculation results based on a model [9]		calculation results – calculation results based on a model [9]	
	For a tractor	For a trailer	For a tractor	For a trailer	For a tractor	For a trailer
The maximum difference with reference to the maximum value, in the steady state	4%	7%	6%	4%	5%	5%
The average difference with reference to the average value, referring to the complete run	3%	21%	4%	8%	6%	21%
The average difference with reference to the average value, in the steady state	2%	4%	2%	2%	2%	3%

4. The crash models

The methods of modelling the vehicle crashes that are presented below take into account the changes of the force that appear during the crash and its influence on the vehicle motion. It is particularly important especially in a crash of articulated vehicles [6], [7].

Two phases of a crash, in crash modelling, are taken into account:

- the first phase – compression – during this phase the value of momentary impact force increases,
- the second phase – restitution – during this phase the value of momentary impact force decreases.

According to Newton hypothesis, these phases are connected by restitution coefficient “ k ”. This coefficient determines which part of the impact energy of compression phase will be regained in the restitution phase. When $k = 1$, ideal spring crash occurs. When $k = 0$, ideal plastic crash occurs. In general, the value of coefficient “ k ” may be taken from interval $[0,1]$. When $k \in (0,1)$ the crash is of spring-plastic type.

For compression and restitution phases, the force impulse can be expressed as:

$$\vec{S}_k = \int_{t_0}^{t_k} \vec{F}(t) dt, \quad (1)$$

where:

\vec{S}_k – force impulse of compression phase,

t_0 – time of the beginning of a crash (beginning of the compression phase),

t_k – time of the end of the compression phase,

$\vec{F}(t)$ – momentary impact force.

$$\vec{S}_k = \int_{t_k}^{t_r} \vec{F}(t) dt, \quad (2)$$

where:

\vec{S}_r – force impulse of restitution phase,

t_r – time of the end of crash (the end of restitution phase).

The total force impulse is equal to the sum of \vec{S}_k and \vec{S}_r

$$\vec{S} = \vec{S}_k + \vec{S}_r. \quad (3)$$

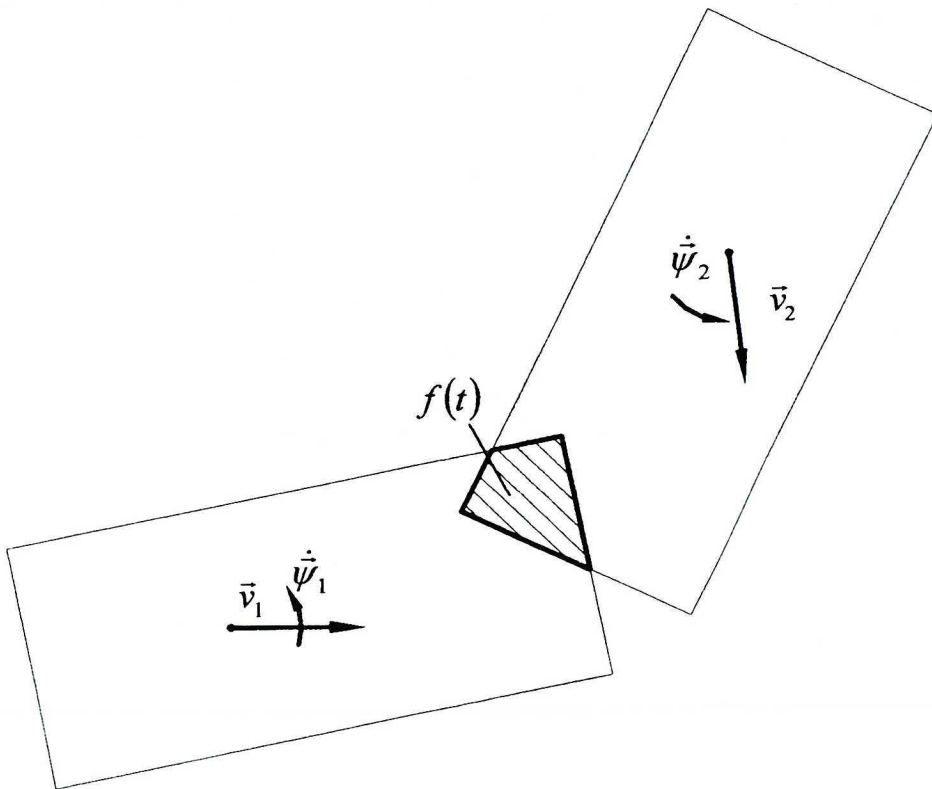


Fig. 9. Crash area

The values of both impulses are connected by restitution coefficient

$$S_r = kS_k. \quad (4)$$

The value of the momentary impact force, during compression phase, which is proportional to the volume of vehicles parts overlapping each other, was accepted in this method of modelling (Fig. 9):

$$F(t) = c f(t), \quad (5)$$

where:

c – stiffness coefficient of the crash area,

$f(t)$ – the crash area.

It is a mean value for the whole crash, and the changes of dimension of the crash area in vertical direction are not taken into account.

By linearizing the course of the impact force in compression and restitution phases, it is possible to present the creation of the impact force as in Figure 10.

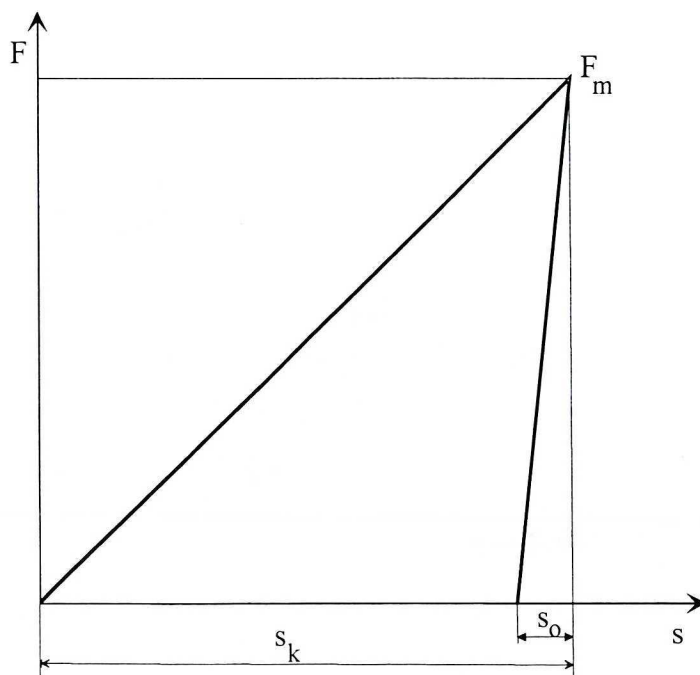


Fig. 10. The impact force in compression and restitution phases

If we take into consideration the mean value of impact force in compression and restitution phases, we can express the restitution coefficient as:

$$kF_{kmid}t_k = F_{omid}t_o, \quad (6)$$

where:

F_{kmid} – mean value of impact force in compression phase,

F_{omid} – mean value of impact force in restitution phase,

t_o – time of restitution phase,

t_k – time of compression phase.

For uniformly variable motion:

$$s_x = \frac{at_x^2}{2}. \quad (7)$$

where:

s_x – length of deformation.

s_x is the mean value of deformation depth measured from the vehicle contour to the centre of gravity of deformation area.

When such an assumption is accepted, the run of impact force in restitution phase can be express as:

$$F(t) = F_m \left(1 - \frac{1}{k^2} \left[1 - \frac{s(t)}{s_k} \right] \right). \quad (8)$$

F_m – maximum value of impact force,

s_k – length of deformation at the end of compression phase.

On the basis of vehicle motion equations and crash equations, a computer program was worked out. In this program two methods of crash modelling were implemented, the first for the vehicles crash, the second for a vehicle crash into an obstacle.

The way of determining the direction of the momentary impact force and the point of its fixing are the main differences in the applied methods.

It was accepted that $\vec{F}(t)$, the vector of the momentary impact force is fixed to the center of gravity of the volume of the parts of vehicles overlapping each other. This point is denoted as C in Figure 11. In the local movable coordinate system, the position of point “ C ” is determined by \vec{r}_1^C vector for “1” vehicle.

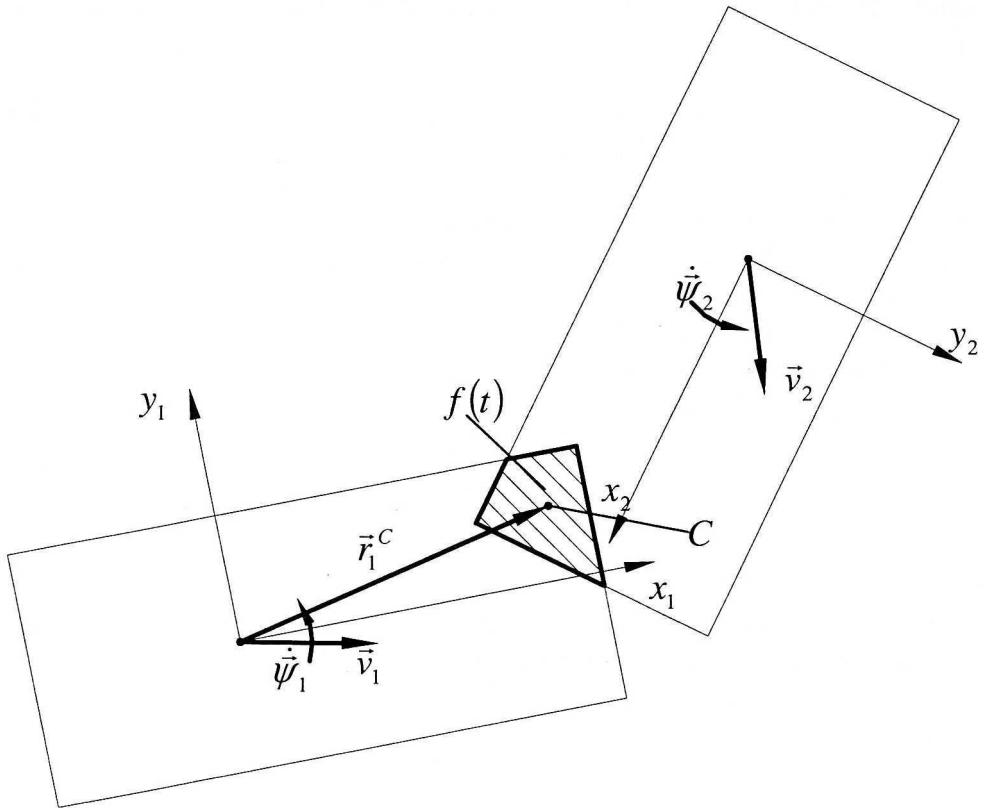


Fig. 11. The diagram of the first method for calculation the vehicles crash

For determining the direction of the momentary impact force we assumed that it acts in the direction which is determined by the difference between the velocity vectors of the vehicle in the impact point (Fig. 12).

These vectors can be expressed as:

- for the first vehicle:

$$\vec{v}_1^C = \vec{v}_1 + \dot{\vec{\psi}}_1 \times \vec{r}_1^C, \quad (9)$$

- for the second vehicle:

$$\vec{v}_2^C = \vec{v}_2 + \dot{\vec{\psi}}_2 \times \vec{r}_2^C, \quad (10)$$

where:

\vec{v}_i^C – the velocity of “i”-vehicle in point C,

\vec{v}_i – the velocity of “ i ”-vehicle,

$\dot{\psi}_i$ – yaw velocity of “ i ”-vehicle,

r_i^C – vector designating C point position in local coordinate system for “ i ”-vehicle.

The unit vector determining the direction of the momentary impact force of the vehicle number 2 can be obtained from the following equation:

$$\vec{e}_2 = \frac{\vec{v}_1^C - \vec{v}_2^C}{\left| \vec{v}_1^C - \vec{v}_2^C \right|}. \quad (11)$$

That is why the vector of the momentary impact force of the vehicle number 2 is expressed as:

$$\vec{F}_2(t) = F(t) \vec{e}_2. \quad (12)$$

The force acting on vehicle number one is the same but sense of a force vector is opposite

$$\vec{F}_1(t) = - \vec{F}_2(t). \quad (13)$$

The momentary impact force is calculated using the above method in compression phase only, and if the value of difference of vehicles velocities is greater then the assumed value:

$$\left| \vec{v}_1^C - \vec{v}_2^C \right| > v_{\min}. \quad (14)$$

This condition prevents the rapid changes of force direction at the end of compression phase when the relative velocity is small.

The force direction during the crash changes in each step of integration, till relative velocity is smaller than the assumed limit, then the force direction of the crash is “stopped” (to avoid the indeterminacy close to the zero velocity).

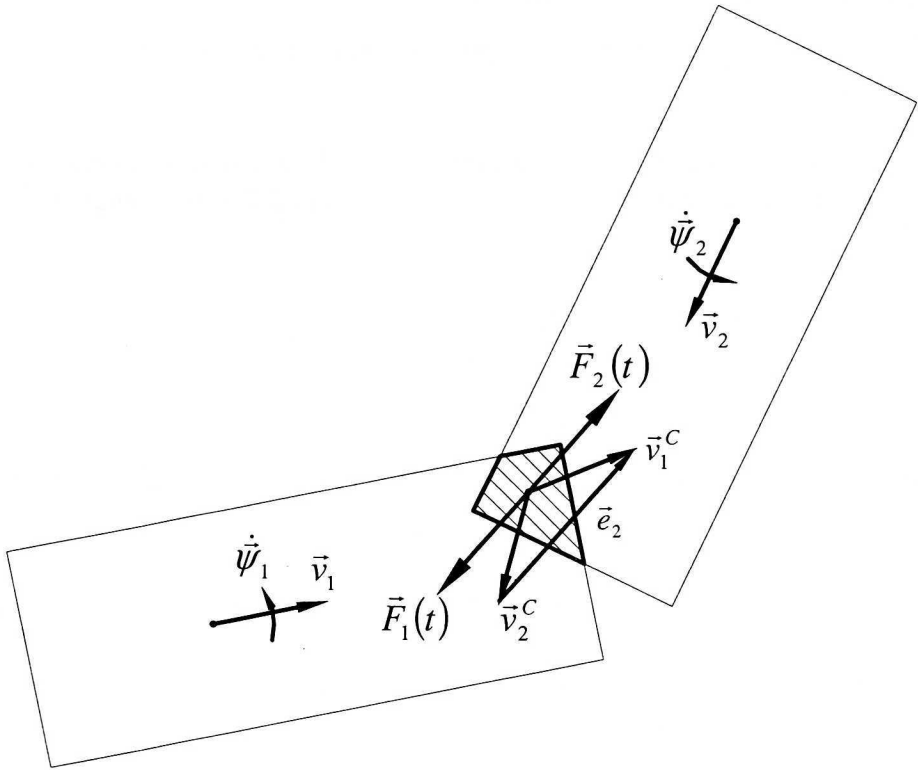


Fig. 12. The momentary impact force for the first method

The second method of crashes calculation.

It is assumed that one of the elements in contact is undeformable, making it possible to simulate collision between a vehicle and an obstacle such as a pole or a wall.

The vector of momentary force is fixed to the point located on the edge of the undeformable obstacle. The point denoted as C is placed half-way of the length from the edge of the stationary obstacle situated in the crash area (Fig. 13).

In the local movable coordinate system, the position of point "C" is determined by \vec{r}_1^C vector for "1" vehicle.

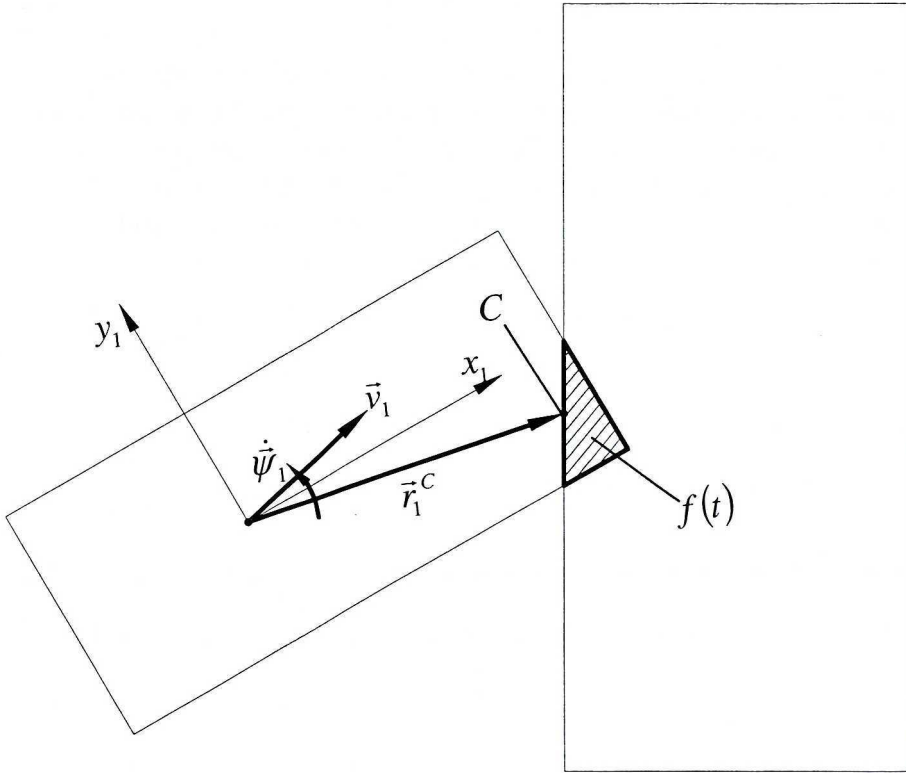


Fig. 13. The diagram of the second method for calculation vehicles crash

The momentary impact force is represented by two components: normal and tangent to the surface of undeformable area.

The action direction of the momentary force is designated as perpendicular to the surface of undeformable area at its connecting points.

The unit vector determining the direction of normal momentary impact force of the vehicle number 1 is marked as \vec{e}_{n_1} in Figure 14.

The vector of normal momentary impact force of the vehicle number 1 is expressed as

$$\vec{F}_1(t) = F_n(t) \vec{e}_{n_1}, \quad (15)$$

where $F_n(t)$ – value of normal component of momentary impact force according to Eq. (5).

Apart from the normal component of momentary impact force, the tangent component $\vec{F}_T(t)$, which can be treated as the friction force appearing

in the crash point, occurs in the crash model. The value of the tangent component can be determined by the difference between velocities of elements in the crash point C. In Figure 14, symbol δ designates the angle between the direction of normal component, and the direction of the difference between velocities. The value of the tangent component cannot be larger than the value of normal component multiplied by friction coefficient μ . Finally, the value of tangent component is designated as follows:

$$\begin{aligned} F_{T_1} &= F_{n_1} \tan \delta, & \text{when } F_{n_1} \tan \delta \leq F_{n_1} \mu, \\ F_{T_1} &= F_{n_1} \mu, & \text{when } F_{n_1} \tan \delta > F_{n_1} \mu, \end{aligned} \quad (16)$$

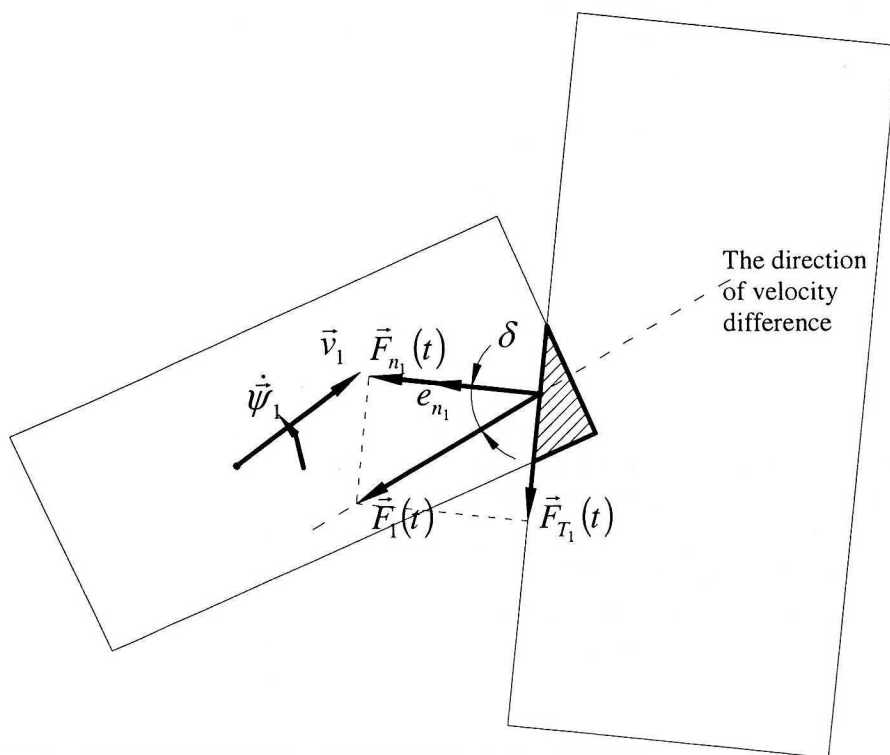


Fig. 14. The momentary impact force for the second method

In both methods, the compression phase ends when the impact area $f(t)$ stops to increase. At that time the restitution phase begins. In this phase, the value of momentary impact force decreases from a maximum value to zero (assuming

assuming that the change of momentary impact force is a linear function of time and depends lineary on the coefficient of restitution).

5. The exemplary simulated crash of articulated lorries

Figure 15 presents the course of simulation of a real crash of a bus and a tractor with semi-trailer. The crash was very well documented [8]. The traces on the road made it possible to determine the place of collision while tachographs plates presented in detail the velocity of the vehicles. Grey colour was used for real situation, black for the simulation results.

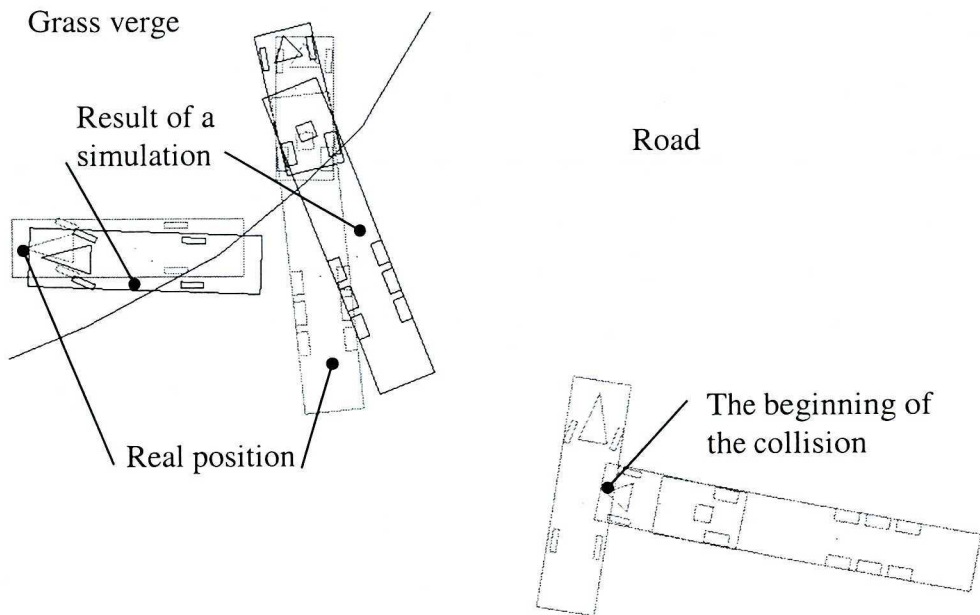


Fig. 15. Simulation of a real crash

The points of the damage may be used for reconstructing the position of a vehicle at the earliest moment of the crash.

6. Conclusions

The mathematical model of a vehicle that was worked out allows us simulate the motion of a conventional vehicle as well as articulated lorries. The presented method of calculating momentary impact force makes it possible to perform the simulation of crashes of articulated lorries. The

comparison of the results of simulation with a real accident showed great similarities.

This work has been supported by the Committee for Scientific Research under the Grant number PB 16/T12/ 2000/18.

Manuscript received by Editorial Board, January 22, 2003;
final version, June 23, 2003.

REFERENCES

- [1] Andrzejewski R.: Stabilność ruchu pojazdów kołowych, WNT, Warszawa, 1997 (in Polish).
- [2] Dugoff H., Fancher P.S., Segel L.: An Analysis of Tire Traction Properties and their Influences on Vehicle Dynamics Performances, SAE Technical Paper 700377.
- [3] Grzeżożek W.: Modelowanie dynamiki samochodu przy stabilizującym sterowaniu siłami hamowania, Z. N. Politechniki Krakowskiej, Seria Mechanika, Monografia Nr 275, 2000 (in Polish).
- [4] Harlecki A.: Metoda analizy dynamicznej mechanicznych układów wieloczłonowych z tarciem suchym w parach kinematycznych, Z. N. Akademii Techniczno-Humanistycznej w Bielsku-Białej, Ser. Rozprawy Naukowe, w druku (in Polish).
- [5] Peterson U. N., Rukgauer A., Schielen W. O.: Lateral Control of a Convoy Vehicle System, Proc. of the 14th IAVSD Symposium held at Ann Arbor, Michigan, USA, August 1995.
- [6] Stefan H., Moser A.: The trailer Simulation model of PC-Crash, Automotive Engineers 1998.
- [7] Stefan H., Moser A.: Accident Reconstruction using optimization strategies, IES Kraków 2002.
- [8] Świder P., Wach W.: Zastosowanie oprogramowania komputerowego dla potrzeb rekonstrukcji wypadków drogowych, Kielce 2002 (in Polish).
- [9] Grzeżożek W., Adamiec-Wójcik I., Wojciech S.: Dynamic analysis of articulated lorries. Conference Proceedings of the 8th Mini Conference on vehicle system dynamics, identification and anomalies, Budapest, November 2002.

Nowe podejście do modelowania zderzeń pojazdów wieloczłonowych

Streszczenie

W artykule zaprezentowano płaski model samochodów wieloczłonowych opracowany dla potrzeb analizy ich dynamiki ruchu. Zastosowano zasadę d'Alamberta dla wyprowadzenia równań ruchu tego systemu. Siły i momenty działające w punkcie styku koła z drogą określono wykorzystując model koła ogumionego opracowany przez Dugoffa i zmodyfikowany przez Uffelmanna. System składa z dowolnej ilości pojazdów połączonych za pomocą par kinematycznych 5-tej klasy (bez tarcia połączenie typu czop-tuleja) oraz siodła w naczepie lub obrotnicy w przyczepie (z tarciem suchym). Ponieważ zazwyczaj zderzenia pojazdów są obliczane wykorzystując impuls siły zderzenia, co nie zawsze pozwala na uzyskanie zadowalających wyników w przypadku pojazdów wieloczłonowych zaprezentowano nowe podejście do obliczania zderzeń. Zaproponowano obliczanie siły w punkcie zderzenia jako funkcji względnej prędkości pojazdów oraz sztywności ich nadwozi. Poddano weryfikacji doświadczalnej przyjęte założenia i uprosz-

czenia w modelowaniu pojazdów wykonując badania drogowe pojazdów wieloczłonowych takich jak ciągnik siodłowy z naczepą oraz samochód ciężarowy z przyczepą. Poddano również weryfikacji zaproponowaną metodę obliczania zderzeń poprzez porównanie położenia pojazdów z bardzo dobrze udokumentowanego zderzenia z położeniem wynikającym ze zrealizowanej symulacji.